Journal of Applied Surfaces and Interfaces 1 (1-3) (2017) 1-6

Journal homepage: http://revues.imist.ma/?journal=jasi

ISSN: 2550-4800

https://doi.org/10.48442/IMIST.PRSM/jasi-v1i1-3.8667

JASI JOURNAL OF APPLIED SURFACES AND INTERFACES

Structural, electronic and optical properties of double perovskite oxide $BaSrMgTeO_6$

M. Ait Haddouch[1,], A. Abbassi[2], Y. Aharbil[1], H. Labrim[3], Y. Tamraoui[4,5], F. Mirinioui[4], A. Benyoussef[2,6], L. Laânab[7] and S. Benmokhtar[1]*

[1] *Laboratoire de Chimie Physique des Matériaux LCPM, Faculté des Sciences Ben M'Sik, Casablanca, Morocco.*
[2] *Laboratoire de Magnétisme et Physique des Hautes Energies L.M.P.H.E. URAC 12, Université Mohammed V, Faculté des Sciences, B.P. 1014, Rabat, Morocco.*
[3] *Centre National de l'Energie, des Sciences et des Techniques Nucléaires, Rabat, Morocco.*
[4] *Univ. Hassan 1er, laboratoire des Sciences des Matériaux, des Milieux et de la modélisation (LS3M),25000, Khouribga, Morocco.*
[5] *Materials Science and Nano-engineering Department, Mohammed VI Polytechnic University, Ben Guerir, Morocco*
[6] *Institute of Nano-materials and Nanotechnologies, MAScIR, Rabat, Morocco.*
7 *Laboratoire Conception et Systèmes (LCS), Université Mohammed V, Faculté des Sciences, B.P. 1014, Rabat, Morocco.*

Received 01 May 2017; Revised 26 June 2017; Accepted 15 July 2017.

Abstract: *A double perovskite $BaSrMgTeO_6$ has been synthesized and characterized by physical techniques: X-ray diffraction, and diffuse reflectance spectroscopy. It crystallizes at room temperature, in the cubic system with unit cell parameters: a=8.018Å (S.G Fm-3m) and shows an almost perfect ordering between Mg^{2+} and Te^{6+} cations at the B substructure. Based on Density Functional Theory (DFT), and using full Potential-linearized Augmented Plane Wave (FP-LAPW) method with the Generalized Gradient Approximation (GGA), implemented in the Wien2k package, we have investigated electronic and optical properties of such material. The optical band gap obtained with GGA approximation is equal to 2.8 eV, which is in good agreement with our experimental results. We found that transmittance T is stable and reaches the average of 90% in both experimental and theoretical studies.*

Keywords: *Synthesis, DFT, Optical properties, Wien2K, band structure, optoelectronic.*

1. Introduction

Ternary compounds of the formula ABX_3, has a large cation at a twelve-coordinated A site, a smaller cation at an octahedrally-coordinated B site, and an anion X, which most often is oxygen. The BX_6 octahedra form a corner-shared network, with remaining voids filled by the cation A. Importantly, the BX_6 octahedra can expand/contract and tilt in order to compensate for non-ideal ionic size ratios.

Perovskite structure is among the most intensely studied materials in solid state chemistry and physics [1]. Perovskites exhibit several fundamentally interesting chemical and physical properties; they can have electronic structures ranging from insulating to metallic, and even half-metallic with spin-polarized electrical conductivity [2,3]; they can show superconductivity [4]; they have magnetic orderings ranging from antiferromagnetic to ferri- and ferromagnetic [5], but can also show magnetic frustration with no apparent long-range order [6,7]; they can show ferroic atomic displacements [8], ionic conductivity [9] and catalytic properties [10]. What is more, perovskites may have many of these properties simultaneously, allowing for new combined properties, such as multiferroicity [11]. As a result, perovskite materials are also of great technical interest, with a range of possible applications such as dielectrics or piezoelectrics in electronic devices and sensors [1], magnetic memory components [3], electrode and electrolyte materials for fuel cells [12], and components for solar cells [13].

The perovskite family is further extended by substitutions, particularly of the A- and B-site cations. These substitutions can result in significant structural distortions that are not only interesting crystallographically but are also important since the distortions can have a critical influence on the electronic and magnetic properties of the perovskite materials [14].

double perovskites of the type $AA'BB'O_6$ are derived from ABO_3 perovskites when half of the 12 coordinated A-site cations and six coordinated B-site cations are replaced by suitable A' and B' cations, respectively.

Some of the insulating/semiconducting $AA'BB'O_6$ compounds could have photocatalytic properties. In the case of photocatalytic compounds, adjusting the band gap and band energies is of importance for the optimization of the optical absorption and redox behavior [15]. In $AA'BB'O_6$ perovskites, the possibility of

* *Corresponding author: E-mail: mohammed.ait.haddouch@gmail.com (Mohammed AIT HADDOUCH)*

combining various cations results in a wide range of different band gaps in the range of 0-5 eV.

The ordered perovskites Ba_2MgTeO_6 and Sr_2MgTeO_6 have also attracted interest as a consequence of their dielectric resonator properties.

To the best of our knowledge, there are no theoretical reports on the electronic and optical properties of $BaSrMgTeO_6$ in the literature. Consequently, the primary purpose of this work is to provide some additional information to the existing data on the physical properties of $BaSrMgTeO_6$ with ab initio calculations. The aims of this work are to synthesis $BaSrMgTeO_6$ and examine the electronic band structure, with emphasis on its derived properties. The calculations are performed using ab initio full-potential linearized augmented plane wave (FP-LAPW) scheme within GGA approach.

2. Experimental

2.1. Sample preparation

A high-quality polycrystalline sample of $BaSrMgTeO_6$ [16] was prepared by a conventional solid-state sintering procedure. $BaCO_3$ (Aldrich, 99.98%), $SrCO_3$ (Aldrich, 99.98%), MgO (99.9%) and TeO_2 were used as starting materials. Appropriate amounts with respect to metal ratios were mixed and thoroughly milled in an agate mortar. The mixed powder was placed in an alumina crucible and calcined at (600 °C/24 h) in an Oxygen environment. After this initial calcination, the sample was heated up at 800 °C/24 h, and 1100 °C/24 h) with several intermediate grindings.

2.2. X-ray powder diffraction pattern analysis

The phase identification and purity of the powder sample were checked from X-ray powder diffraction (XRPD) patterns. The XRPD data for Rietveld analysis were collected at room temperature on a D2-Phaser diffractometer (Ge monochromatized Cu Kα radiation, Bragg-Brentano geometry) in the 2θ range 10-100° with a step size of 0.02° (the counting time was 15 s per step). The slit system was selected to ensure that the X-ray beam was completely within the sample for all 2θ (°) angles.

2.3. Optical properties

The optical properties of double perovskite $BaSrMgTeO_6$ have been carried out using a Perkin Elmer Lembda900 Spectrophotometer and have been recorded at room temperature in the region 200–2000 nm.

3. Results and discussion

3.1. Structural analysis

Fig.1 shows the X-ray powder diffraction (XRPD) profile of $BaSrMgTeO_6$. The continuous curve corresponds to the calculated pattern obtained from Rietveld refinement and the symbols represent the experimental data. A pseudo-Voigt function was used to describe individual line profiles. After an appreciable profile matching the position parameters and isotropic atomic displacement parameters of individual atoms were also refined. An excellent fit of calculated and observed XRPD was achieved. The bottom curve is the difference between the experimental and calculated patterns. Note that a very small quantity of Magnesium Tellurate $MgTeO_4$ as an impurity was detected in the sample and indicated by (*). Good agreement between the observed and calculated interplaner spacings (d-values) suggests that the compound crystallizes in cubic symmetry with $Fm\bar{3}m$ as space group, as was originally reported by Tamraoui et al [16] at room temperature with cell parameters a= 8.0180(1) Å. The similarities in the cell parameters of $BaSrMgTeO_6$ and Ba_2MTeO_6 (M = Ca, Cd, Mg) (Table 1) suggest that the compounds are isostructural. The structural data obtained from the refinement are given in Table 2.

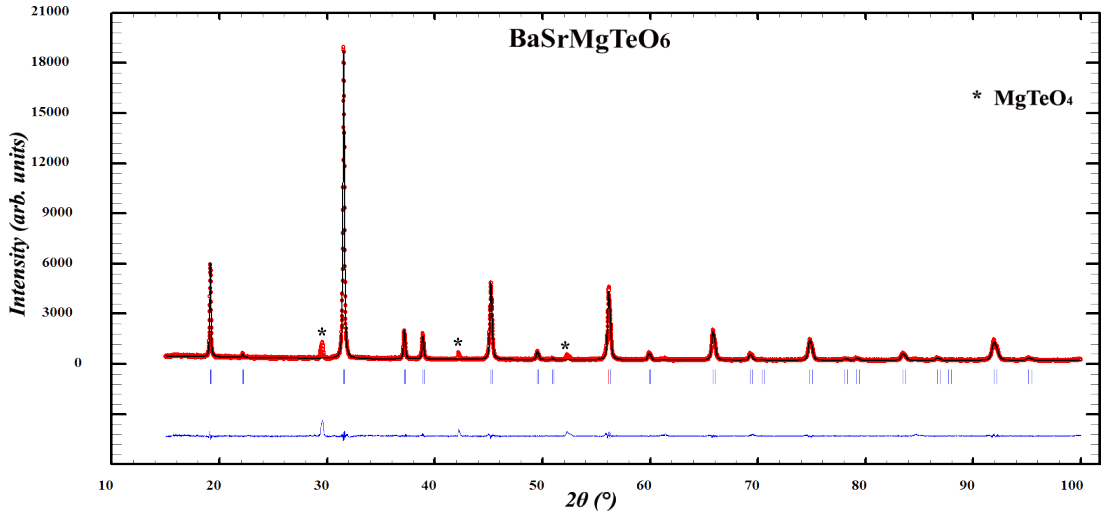

***Fig.1**. Final Rietveld plots for the cubic $BaSrMgTeO_6$. The upper symbols illustrate the observed data (circles) and the calculated pattern (solid line). The vertical markers show calculated positions of Bragg reflexions. The lower curve is the difference diagram.*

The analysis of refined crystallographic parameters in $BaSrMgTeO_6$ indicates that the Mg^{2+} and Te^{6+} are octahedrally coordinated with the oxygen atoms. The $[MgO_6]$ and $[TeO_6]$ octahedra are alternatively connected and extended in three dimensions. The O atoms connect the $[MgO_6]$ and $[TeO_6]$ octahedra along the three directions. The typical Mg-O-Te bond angle constrained to 180° by space group Fm-3m and O position coordinates (0.2614, 0, 0), indicating no tilt with respect to a, b and c-axes. A (0 0 1) projection of the $BaSrMgTeO_6$ unit cell indicating the typical polyhedral arrangement is shown in Fig.2.

Table 1

Comparison of the cell parameters of the double perovskite-type.

Ba_2MTeO_6	Space group	a(Å)	Ref.
$Ba_2CaTe\ O_6$	$Fm\bar{3}m$	8.390	**[17]**
$Ba_2CdTe\ O_6$	$Fm\bar{3}m$	8.360	**[17]**
$Ba_2MgTe\ O_6$	$Fm\bar{3}m$	8.130	**[17]**
$BaSrMgTeO_6$	$Fm\bar{3}m$	8.018	this work

Table 2

XRPD fitting and structural parameters

Atom	Site	X	y	Z	
Ba^{2+}/Sr^{2+}	8c	¼	¼	¼	
Mg^{2+}	4b	½	½	½	
Te^{6+}	4a	0	0	0	
O	24e	0.2614	0	0	R_F= 2.88 R_B= 2.54 R_p= 4.84 Rwp=7.20
6 × Te–O		1.913	12 × O–Te–O	180	
6 × Mg–O		2.095	3 × O–Te–O	90	
12 × (Ba/Sr) –O		2.836			

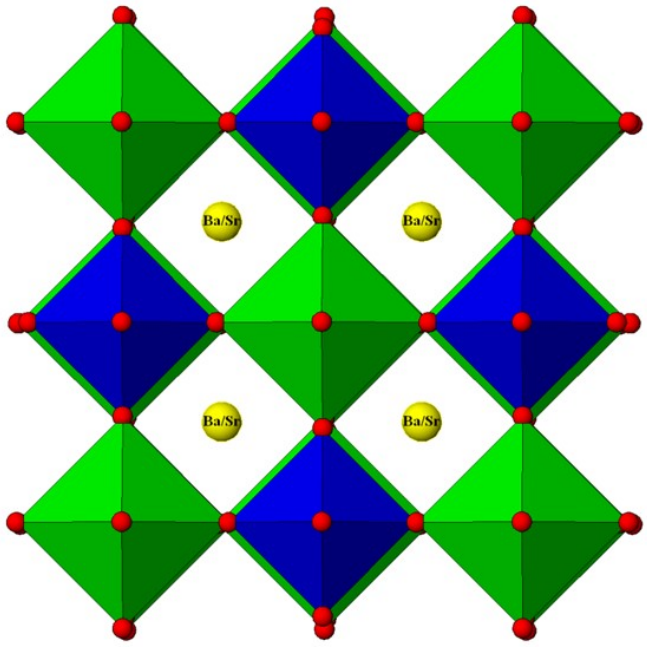

Fig.2*. 3D view of the cubic crystal structure of double perovskite oxide $BaSrMgTeO_6$ with 1:1 ordering of two different cations (space group Fm-3m), the yellow and red spheres represent the Ba^{2+}/Sr^{2+} and O^{2-} ions, respectively. The view showing the corner-sharing MgO_6 (green octahedral) and TeO_6 (blue octahedral) in straight angle (<Mg–O–W>=180°) with Ba^{2+}/Sr^{2+} cations residing in the cavities formed by the octahedral network.*

3.2. Band Gap study by UV-visible Spectroscopy

The UV–vis absorption spectrum of $BaSrMgTeO_6$ is shown in Fig.3. The energy band gap is determined using absorption spectrum with the help of Tauc relation [18, 19] given by

$$\alpha h\nu = A(h\nu - Eg)^n$$

Where hv is the energy of the incident photon, α is the absorption coefficient, and A is a characteristic parameter independent of the photon energy, Eg is the optical band gap and the value of n is 1/2 or 2 for the direct or indirect transition respectively. Using this relation, a graph is plotted between $(\alpha h\nu)^2$ and hv as shown in Fig.3. The extrapolation of the linear absorption edge part of this graph with a straight line to $(\alpha h\nu)^2 = 0$ axis gives the value of the band gap. The value of the optical band gap of the material for direct transition is found to be ~2.8eV.

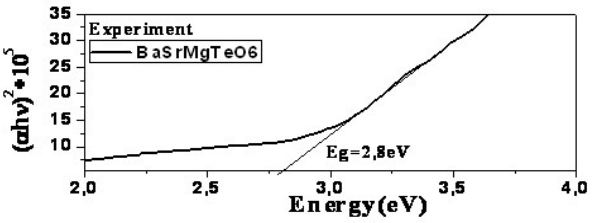

***Fig.3**. UV–vis absorption spectrum for direct transition ($(\alpha h\nu)^2$ vs. hv).*

3.3. Computational details

The electronic and optical properties of $BaSrMgTeO_6$ are investigated using the Full Potential Linearized Augmented Plane Wave method implemented in Wien2K code [20]. The structure information for theoretical calculations was obtained from the Rietveld refinement of powder X-ray diffraction data obtained for the $BaSrMgTeO_6$ ceramic in our experimental study. This calculation was performed using the Generalized Gradient Approximation (GGA) [21] for the exchange-correlation potential, the used energy cutoff is −8.0 Ryd for the LAPW. We work with 1000K-point and our self-consistent was stable at 10^{-6}Ryd.

3.4. Electronic properties

Fig.4 shows the total and partial density of state(Tdos,Pdos) of $BaSrMgTeO_6$ compound, we proceed this calculation in order to understand the electronic configuration of this material. The total density of state shows the existence of different bands in different regions. The conduction band of $BaSrMgTeO_6$ consists essentially of different states of Ba, Sr, and Mg. We note that the d states of Ba, d states of Sr, s and p states of Mg which are in hybridization from 5ev to 10 ev contribute to the appearance of BC.

The valence band consists of several regions and important peaks. The peak noticed at E = -14.7ev is due mainly to the contribution of p states of Sr and the peak located in the area between -10.4ev and -8.2ev is mainly due to p states of Mg, the p states of Mg are weakly hybridized with p states of Ba.The theoretical calculation made shows also an appearance of a strong and broadband between -5eV and 0ev, which is mainly due to a strong hybridization between p states of oxygen and p states of Mg, we also note that the s states of Mg contribute to the appearance of this region.

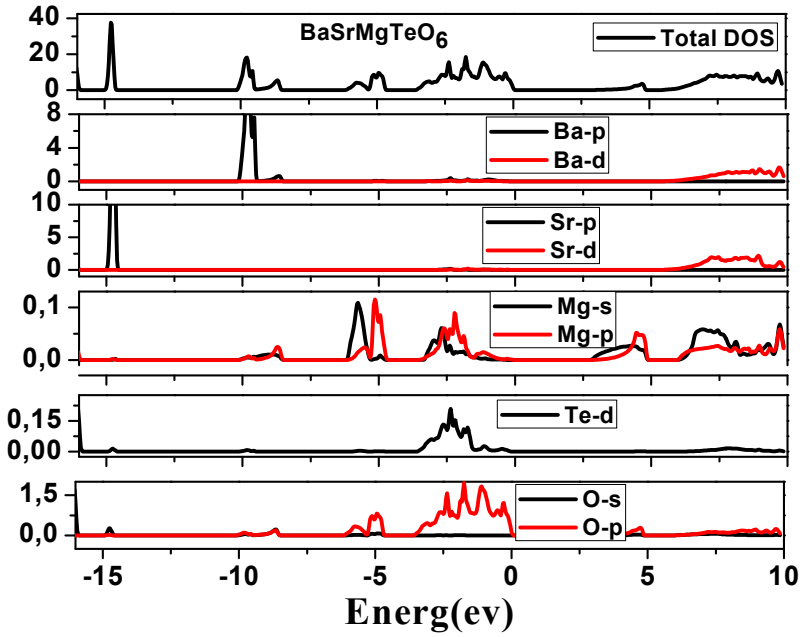

***Fig.4.** The total and partial density of state of $BaSrMgTeO_6$ compound.*

According to Fig. 4, the energy difference between the top of the valence band and the bottom of the conduction band corresponds to a charge transfer between the p states of oxygen and Mg states, these states explains the origin of the band gap found in the experimental results

In this present work, we have also determined the band structure of the studied material. Based on the analysis of transitions between the conduction band and valence band, the band structure can show the nature of the gap found if it is direct or indirect. According to Fig.5, the maximum of the valence band and the minimum of the conduction band correspond to a direct transition at Γ point which shows that the gap of $BaSrMgTeO_6$ material is direct, the gap values found with the GGA approximation is equal to 2.64 eV which is very close to the experimental value(Eg=2.8eV). Based on the absorption spectrum we will investigate the optical band gap for more precision concerning the gap value.

3.5. Optical properties: Theoretical and experimental study:

According to the Fig.5, the band structure presented show that the band gap is direct, thus m will take 2 and the optical band gap will be found in the plot of $(\alpha h\nu)^2$ versus $(h\nu)$.

Fig.6, show the optical band gap in both experiment and theoretical investigations, the experiment value found is equal to 2.8 eV. The theoretical spectrum of absorption show that the value found is the same as in experiment one, thus the transfer of charge explained in PDOS correspond to the value of 2.8eV.

Fig.7 shows the optical transmittance of $BaSrMgTeO_6$ compound which is calculated based on the absorption measured using the Beer-Lambert. This experimental result was verified by a theoretical calculation. We note that the transmittance spectrum reaches the average value of 90% in the visible light region. This means that this material is highly transparent, a much lower amount of hv radiation is absorbed by the material. It should also be noted that the calculation has been done confirmed the experimental result and shows that $BaSrMgTeO_6$ is very transparent. Such materials can be thus exploited in optoelectronic and photovoltaic applications for their importance as transparent materials and alternative candidates for ITO [22].

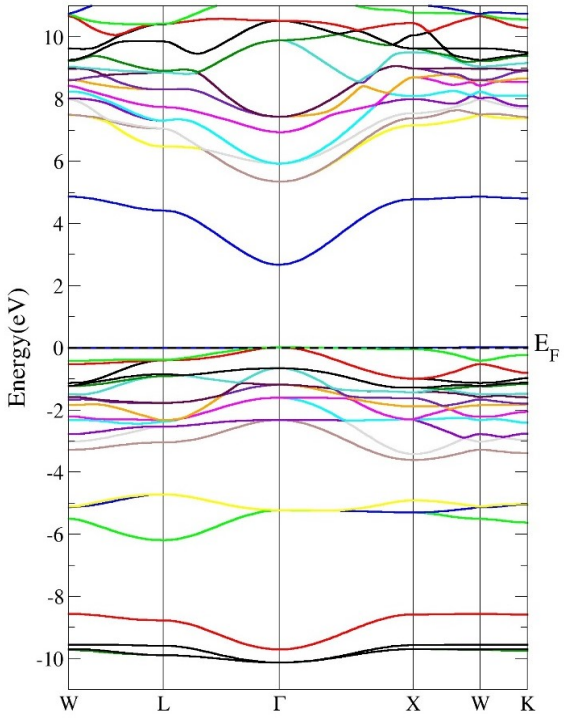

***Fig.5**. Band structure of BaSrMgTeO6 compound*

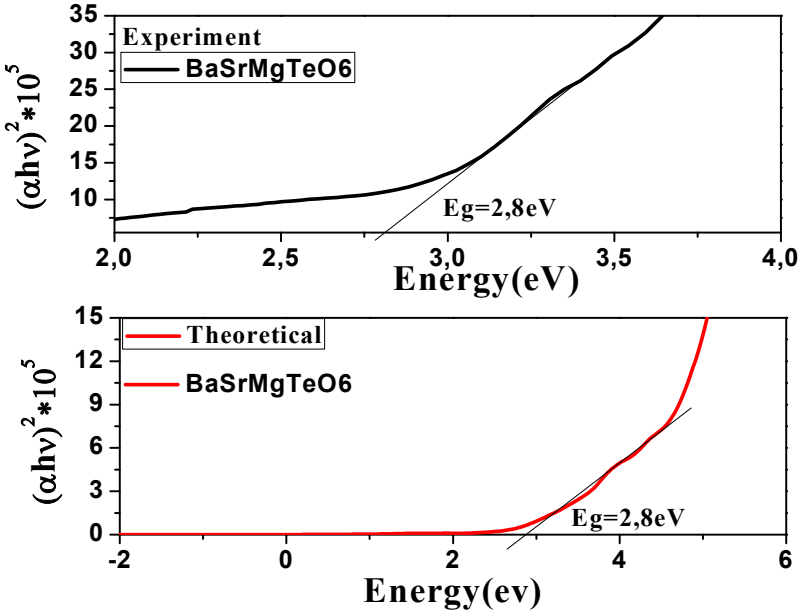

***Fig.6.** The optical band gap*

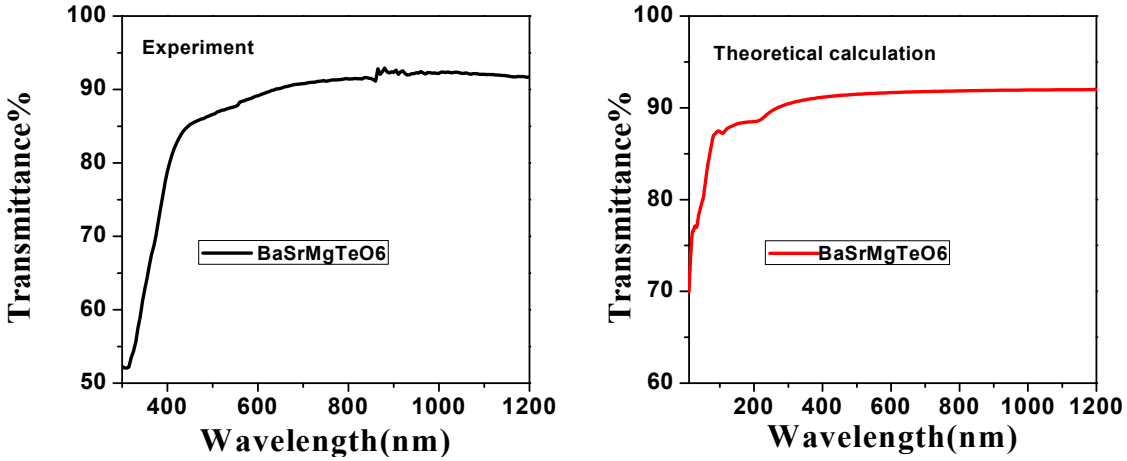

***Fig.7**. The optical transmittance of $BaSrMgTeO_6$: experiment and theoretical study*

4. Conclusion

Double perovskite $BaSrMgTeO_6$ ceramic was prepared by solid state reaction method. Rietveld refinements showed that the sample crystallized with cubic ($Fm\bar{3}m$) symmetry.

First-principles calculations based on FP-LAPW method with generalized gradient approximation (GGA) was used to calculate the electronic and optical properties of double perovskite $BaSrMgTeO_6$. The calculations show that optical gap obtained is direct and close to the experimental data which is equal to 2.8ev.

The theoretical and the experimental studies show that the absorption is high in the ultraviolet and shift to the low values, $BaSrMgTeO_6$ doesn't absorb the radiation (hv) in the range of visible light and from λ=800 nm the absorption becomes very low. The transmittance T is stable and reaches the average of 90% in both experiment and theoretical studies. We showed significant agreement between results of calculations by First principle and the existing experimental data, this result confirms the characteristic that can present $BaSrMgTeO_6$ to be used as suitable transparent material electrodes in solar cells.

References

[1] A.S. Bhalla, R. Guo, R. Roy, Mater. Res. Innov. 4(1) (2000) 3-26.
[2] W.E. Pickett, D.J. Singh, Phys. Rev. B 53(3) (1996) 1146-1160.
[3] K.-I. Kobayashi, T. Kimura, H. Sawada, K. Terakura, Y. Tokura, Nature 395 (1998) 677-680.
[4] R.J. Cava, B. Batlogg, J.J. Krajewski, R. Farrow, L.W. Rupp, A.E. White, K. Short, W.F. Peck, T. Kometani, Nature 332 (1988) 814 - 816.
[5] J.B. Goodenough, J.M. Longo Physics. Vol. 4: Magnetic and Other Properties of Oxides and Related Compounds, Part a, Springer, Berlin, 1970, pp. 126-367.
[6] P.D. Battle, T.C. Gibb, C.W. Jones, F. Studer, J. Solid State Chem. 78 (1989) 281-293.
[7] C.R. Wiebe, J.E. Greedan, P.P. Kyriakou, G.M. Luke, J.S. Gardner, A. Fukaya, I.M. Gat-Malureanu, P.L. Russo, A.T. Savici, Y.J. Uemura, Phys. Rev. B 68 (2003) 134410.
[8] N.A. Benedek, C.J. Fennie, J. Phys. Chem. C 117(26) (2013) 13339-13349.
[9] M. Li, M.J. Pietrowski, R.A. De Souza, H. Zhang, I.M. Reaney, S.N. Cook, J.A. Kilner, D.C. Sinclair, Nat. Mater. 13(1) (2014) 31-35.
[10] H. Tanaka, M. Misono, Curr. Opin. Solid State Mater. Sci. 5 (2001) 381-387.
[11] S.-W. Cheong, M. Mostovoy, Nat. Mater. 6 (2007) 13-20.
[12] Y.-H. Huang, R.I. Dass, Z.-L. Xing, J.B. Goodenough, Science 312 (2006) 254-257.
[13] M.A. Green, A. Ho-Baillie, H.J. Snaith, Nat. Photonics 8(7) (2014) 506-514.
[14] R. H. Mitchell, "Perovskites: Modern and Ancient," Almaz Press, Thunder Bay, Canada, 2002.
[15] H.W. Eng, P.W. Barnes, B.M. Auer, P.M. Woodward, J. Solid State Chem. 175 (2003) 94-109.
[16] Tamraoui Y, Manoun B, Mirinioui F, Haloui R and Lazor P. J. Alloys Compd. 603 (2014) 86-94
[17] S.Vasala, M.Karppinen, $A_2B'B''O_6$ Perovskites: A review, Progress in Solid State Chemistry 43(1-2) (2014) 1-36
[18] J. Tauc, R. Grigorovici, A. Vancu, Phys. Status Solidi 15(2) (1966) 627-637.
[19] E.A. Davis, N.F. Mott, Philos. Mag. 22 (1970) 903.
[20] P. Blaha, K. Schwarz, G.K.H. Madsen, D. Kvasnicka, J. Luitz, WIEN2k, An Augmented Plane Wave + Local Orbitals Program for Calculating Crystal Properties (Karlheinz Schwarz, Techn. Universität Wien, Austria) 2001
[21] J.P. Perdew, K. Burke, et M Ernzerhof, Phys.Rev.Lett., vol. 77(18) (1996) 3865-3868
[22] Seon-Soon Kim, Se-Young Choi , Chan-Gyung Park, Hyeon-Woo Jin, Thin Solid Films 347 (1–2) (1999)155–160